Undulated oxo-centered layers in PbLn_3O_4 (VO_4) (Ln= La and Nd) and relationship with Nd_4O_4(GeO_4)

Marie Colmont, Olivier Mentre, Natacha Henry, Alain Pautrat, Bastien Leclercq, Frédéric Capet, Nora Djelal, Pascal Roussel

Undulated oxo-centered layers in $PbLn_3O_4(VO_4)$ (Ln= La and Nd) and relationship with $Nd_4O_4(GeO_4)$.

Marie Colmont*[1], Olivier Mentré[1], Natacha Henry[1], Alain Pautrat[2], Bastien Leclercq[1], Frédéric Capet[1], Nora Djelal[1] and Pascal Roussel[1]

[1] Univ. Lille, CNRS, Centrale Lille, ENSCL, Univ. Artois, UMR 8181 - UCCS - Unité de Catalyse et Chimie du Solide, F-59000 Lille, France

[2] CRISMAT, CNRS, UMR 6508, ENSICAEN, Caen, France

Email : marie.colmont@ensc-lille.fr

ABSTRACT: Single crystals of $PbLa_3O_4(VO_4)$ have been synthesized using the flux growth technique and characterized by X-ray diffraction. The crystal structure of the tittle phase was solved by charge flipping and refined to $R_1 = 0.024$ ($wR_2 = 0.031$) for 2777 reflections [$I > 3\sigma(I)$]. The compound is orthorhombic and crystallized in the space group *Cmcm*: $a = 5.8686(6)$Å, $b = 17.898(2)$Å, $c = 7.9190(7)$Å, $V = 831.8(1)$Å^3, $Z = 4$. The structure is built on $[PbLa_3O_4]^{3+}$ layers with zig-zag cross-sections, surrounded by isolated $(VO_4)^{3-}$ tetrahedra. Its crystal structure shows direct relationship with the isoformular $Nd_4O_4(GeO_4)$ compound which crystallized in the primitive non centrosymmetric *Pb2$_1$m* sub-group. Its stability in temperature and under air was checked as well as optical properties. In a second part, lanthanum was substituted by neodymium giving rise to a paramagnet and f→ f electronic excitations superposed to the broad absorption front below 3.05eV related to the presence of VO_4 groups.

Keywords: Lanthanum; Lead; Vanadium; Oxo-centered tetrahedra, Flux growth synthesis; Crystal structure, Optical and magnetic properties

Introduction

The search for new luminescent materials is a hot topic of today's solid state chemistry. Indeed, it is of necessity to save energy through the replacement of light bulbs with LED-based solid-state white lighting. Most of the actual commercialized white LEDs are based on the conversion of LED light via inorganic phosphors [1]–[3]. Running towards new advanced materials with high quantum yields and a good thermal stability is on a roll. In this context, lanthanum based oxides are promising because of their ability to host emitters, turning then to phosphors. [4]–[6]

Following the recent discovery of the new $KLa_5O_5(VO_4)_2$ [7] structure and its promising luminescent properties [8], we investigated another ternary system $PbO\text{-}La_2O_3\text{-}V_2O_5$. To the best of our knowledge, the title compound is the first lead, vanadium and lanthanum ternary system. Here, in order to overpass the problem of stability of lanthanum orthovanadate (i.e.$LaVO_4$ [9]) and lead vanadates (i.e. $Pb_3(VO_4)_2$ [10], $Pb_2V_2O_7$ [11]…) currently obtained after heating a mixture of primary oxides, an alternative synthetic flux growth route was used. It is known to be a method of choice to grow original architectures from various compositions. Here PbO was chosen both as flux and a reactant, as proposed in [12], leading to the title compound: $PbLa_3O_4(VO_4)$. This compound appears to be one of the broad series of compounds described using the anion-centered tetrahedra [13] around the four oxo-anions of the above formula. This means that its cationic backbone is built on the association by edges of $O(La/Pb)_4$ tetrahedra. Accordingly to this anti-tetahedra description, vanadates are considered as isolated and surrounding the $[PbLa_3O_4]^{3+}$ polycationic body.

Herein we report on the synthesis and structural characterization of a new lead lanthanum vanadate oxide, and discuss structural relations with the related $Nd_4O_4(GeO_4)$. Then, its structural stability under air at low (100K) and high temperature (until 1073K) was checked. In a second step, the neodymium compound was synthesized bringing f→f electronic transitions and paramagnetism.

Results and Discussion

Single crystals of $PbLa_3O_4(VO_4)$ were grown using the flux growth method, at 900 °C and in a platinum crucible from a mixture of PbO, $La(OH)_3$ and V_2O_5 mixed in a 3 : 1 : 1 molar ratio (see Experimental section below). The crucible was fitted with a platinum lid. It is interesting to note that, due to the refractory behaviour of lanthanum hydroxide, the flux growth technique is often preferred to isolate crystals of novel members [12], [14]. The combined choice of Pb^{2+} and La^{3+} is governed by their matching within oxo-centered tetrahedra (OPb_4) [15] (OBi_4) [16], [17] or (OCu_4) [18]… The "flexibility" induced by highly polarizable lone pair Pb^{2+} species is another key-parameter, this cation

being susceptible of sizeable Pb-O distances and the inherent possibility for mixed oxo-centred units, for example in $O(Pb,Bi)_4$ [19], [20], or $O(Pb,Cu)_4$ [21].

Small orange crystals (0.11 × 0.09 × 0.02 mm^3) of $PbLa_3O_4(VO_4)$ were studied using single-crystal X-ray diffraction analysis (Table 1). The compound crystallizes in the *Cmcm* space group with unit cell parameters: a = 5.8686(6) Å, b = 17.8980(18)Å, c = 7.9190(7)Å, Z = 4, R_1 [$I > 3\sigma(I)$] = 0.0237, GOF = 1.70. The atomic positions, displacement parameters are given in Supplementary Information S1, S2 and S3. The crystal-structure data for $PbLa_3O_4(VO_4)$ phase were deposited with the depository number CSD-431424.

$PbLa_3O_4(VO_4)$ is isotypic with the previously reported $Nd_4O_4(GeO_4)$, [22]. In this compound the ionic mobility of the substoechiometric oxo-centred anions was shown after substitution of $Ge^{4+}$by Ga^{3+}. [23] Selected structural data and main distances for both structures are compared in Table 1.

Table 1. Crystallographic data and selected bond distances (Å) for $PbLa_3O_4(VO_4)$ (**I**), and $Nd_4O_4(GeO_4)$.[22]

	$PbLa_3O_4(VO_4)$	**$Nd_4O_4(GeO_4)$**[22]	
Space group	*C*m*cm*	*Pb*2_1*m*	
a / Å	5.8686(6)	5.727(2)	
b / Å	17.8980(18)	17.927(5)	
c / Å	7.9190(7)	7.475(2)	
V / $Å^3$	831.78(14)	767.4(4)	
Z	4	4	
D_{calc}/g·cm^{-3}	6.409	6.730	
Selected distances in $PbLa_3O_4(VO_4)$ (Å)			
V5-O6x2	1.689(5)	**O5**-La1x	2.481(5)
V5-O2x2	1.751(5)	O5-Pb1x1	2.188(5)
O4-La3x2	2.364(3)	O5-La3x2	2.415(3)
O4-La1x2	2.490(3)		
Selected distances in $Nd_4O_4(GeO_4)$ (Å)			
Ge1-O6x2	1.765	**Ge2**-O8x2	1.733
Ge1-O4	1.777	Ge2-O5x2	1.737
Ge1-O2	1.820	Ge2-O7	1.758
O1-Nd3	2.272	**O3**-Nd3	2.183
O1-Nd5x2	2.275	O3-Nd1	2.417
O1-Nd1	2.416	O3-Nd5x2	2.424
O9-Nd4	2.187	**O10**-Nd6x2	2.280
O9-Nd2	2.284	O10-Nd4	2.284
O9-Nd6x2	2.373	O10-Nd2	2.471
O11-Nd5	2.256	**O12**-Nd5	2.242
O11-Nd2	2.548	O12-Nd1	2.377
O11-Nd1	2.264	O12-Nd6	2.388
O11-Nd6	2.411	O12-Nd2	2.44

The crystal structure of $PbLa_3O_4(VO_4)$ is presented figure 1a), b) and c). It contains one Pb, one V, two La and four O independent sites. It is formed of $O(Pb,La)_4$ anion-centered tetrahedra .i.e. , $O4La1_2La3_2$ ($d_{O4\text{-}La1}$= 2.490(3)Å, $d_{O4\text{-}La3}$= 2.364(3)Å) and O5 $La3_2La1Pb1$ ($d_{O5\text{-}La3}$= 2.415(3)Å, $d_{O5\text{-}Pb1}$= 2.188(5)Å, $d_{O5\text{-}La1}$= 2.481(5)Å). It creates $[PbLa_3O_4]^{3+}$ cationic layers (figure 1d)) surrounded by VO_4 orthovanadates (figure 1e)).

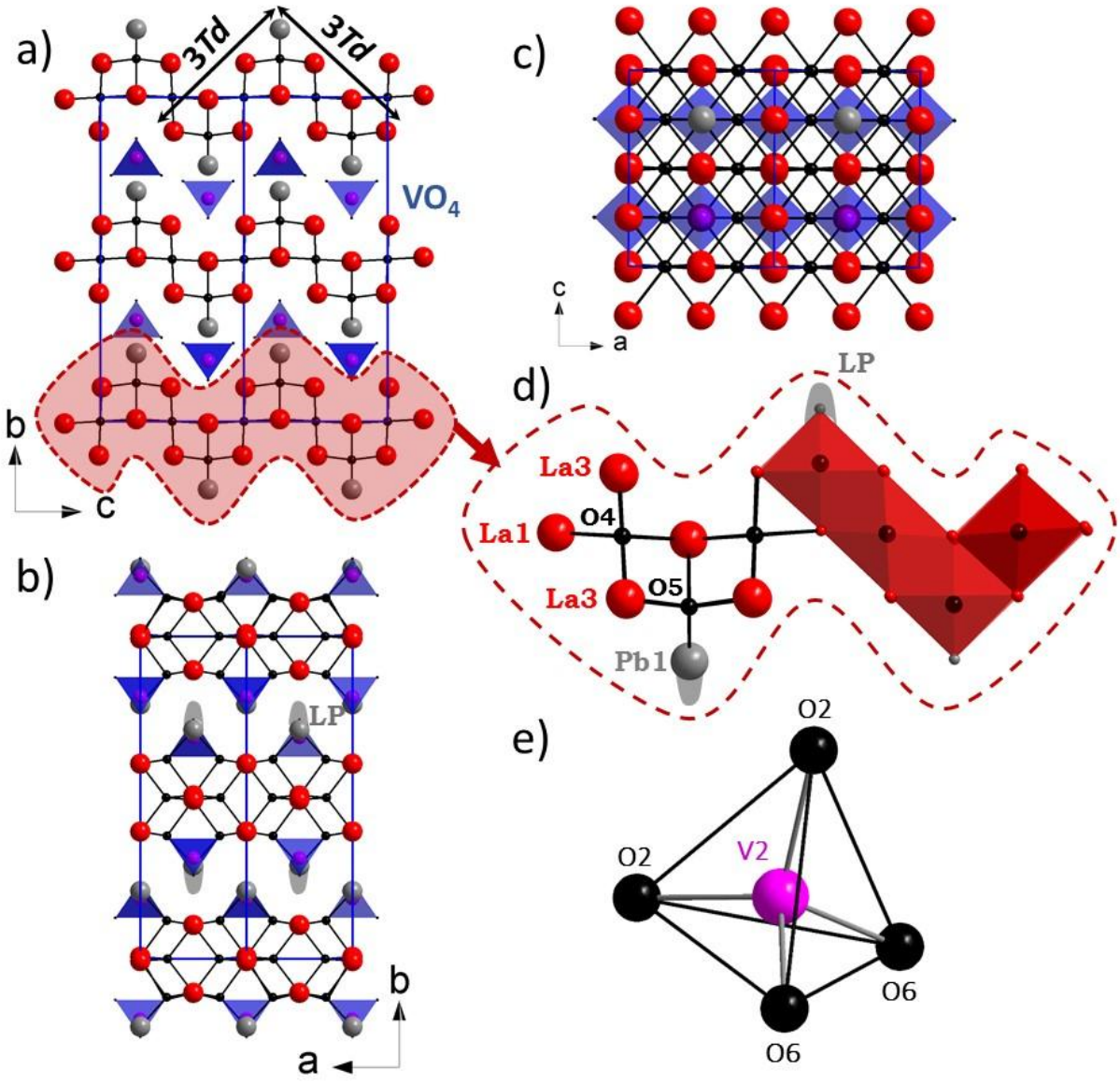

Figure 1. Projection of the crystal structure of $PbLa_3O_4(VO_4)$ a) along *a*-axis, b) along *c*-axis, c) along *b*-axis. It is built on stacking of $[PbLa_3O_4]^{3+}$ zig-zag cationic layers d) surrounded by e) isolated VO_4 tetrahedra. The lone pair of Pb^{2+} are highlighted in dark grey. They point outward the layers, between two V^{5+} cations

$[PbLa_3O_4]^{3+}$ cationic layers are growing parallel to the (a,c) plane, built on the edge-sharing of (OLa_4) and ($OPbLa_3$) tetrahedra and connected according to a zig-zag cross section, with 3 tetrahedra long segments (figure 1a)). The co-presence of La^{3+}/Pb^{2+} in the oxo-centered tetrahedra is extremely rare. To the best of our knowledge this new phase is the second example of a structure hosting such mixed units (i.e. (OPb_3La) and (OPb_2La_2) in Pb_6LaO_7X, X= Cl, Br). [24] It is noteworthy that the La^{3+}/Pb^{2+} ordering located Pb^{2+} at the Cresnel-edge of the zig-zag layers so that its lone pair (LP) is able to point outward between two V^{5+} cations. The position of the lone pair of Pb^{2+} was estimated using the Verbaere and co-workers method as implemented in the HYBRIDE software. [25] This is based on the local electric field *E* calculation in the whole crystal using the Ewald's method.[26] Under the influence of this electric field on the cation center, the lone pair is displaced by an amount *d* deduced by the relation $\mu = q*d = \alpha*E$ with *q* corresponding to the lone pair charge (equal to -2) and μ corresponding to Pb^{2+}-*E* dipolar momentum. We have used Pb^{2+} Shannon polarizability of α= 6.58 $Å^3$. The description of the method is described elsewhere [27], [28]. The results are given Table S1. The refined lone pair coordinates are [0.5, 0.2141, 0.75] corresponding to a Pb-LP distance of about 1.36 Å. This is a realistic value and the LP exactly takes place in the empty space between two VO_4 tetrahedra aligned along *a*-axis (figure 1b)). The geometry of the VO_4 tetrahedron is quite regular with V-O distances ranging between 1.689(5) and 1.751(5)Å and O-V-O angles between 104.2 and 110.5°.

This compound is structurally closed to $Nd_4O_4(GeO_4)$ (figure 2) where La^{3+}, Pb^{2+} and V^{5+} are replaced by Nd^{3+}, another Nd^{3+} and Ge^{4+}.

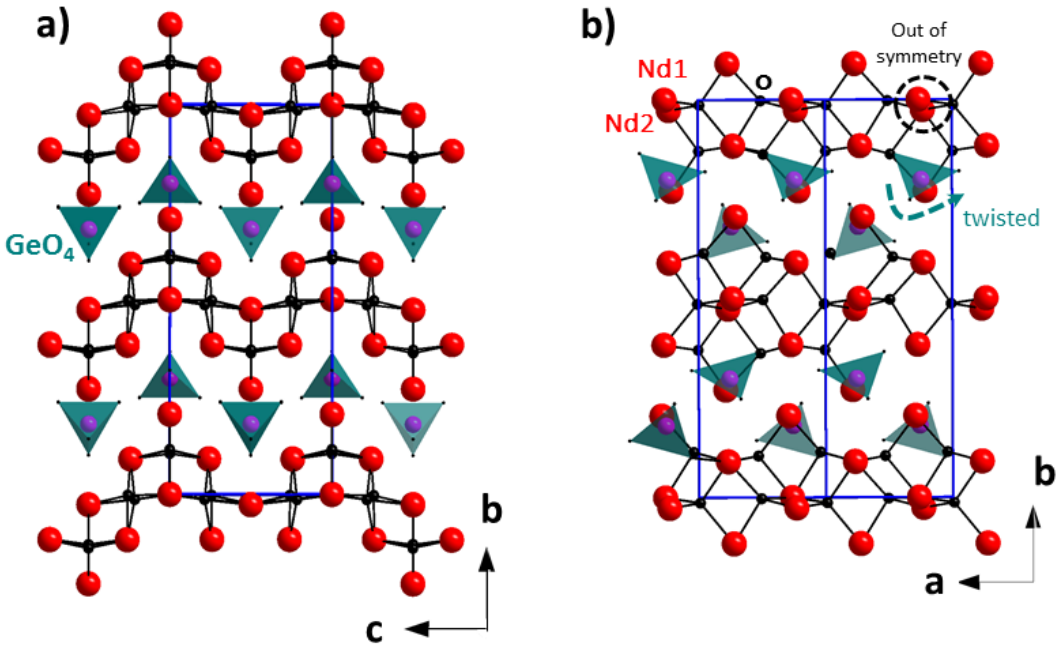

Figure 2. Projections of the crystal structure of $Nd_4O_4(GeO_4)$ [23] along a) *b*- and b) *a*-axis. It is built on the same kind of $[Nd_4O_4]^{4+}$ polycationic layers surrounded by isolated GeO_4. The differences with $PbLa_3O_4(VO_4)$ are highlighted to evidence the reduction of symmetry leading to

a P-Bravais lattice (i.e. Nd1 and Nd2 on crystallographic sites with local symmetry *m* and tilting of GeO_4 tetrahedra).

In the literature, $Nd_4O_4(GeO_4)$ crystal structure was first reported by Merinov et al. [22] in an orthorhombic P-centered unit cell. The cross-substitution of Nd (ionic radius R=0.983Å) by La and Pb (R=1.032Å and 1.19Å, respectively), and Ge (R= 0.39Å) by V (R= 0.355Å), induced significant modifications of the unit-cell volumes (767.44$Å^3$ for Nd compound versus 831.78$Å^3$ for the La counterpart; and symmetries. Oxo-centered structures with counter oxo-anions often display versatile symmetries depending on the size-matching between OM_4 and XO_4 groups. For instance, the $BiM_2O_2(XO_4)$ series show a plethora of distortions [29] sometimes accompanied by large supercell ordering and/or incommensurate modulations tuning the X chemical nature, see the $BiCu_2O_2(V_{1-x}P_xO_4)$ case. [30], [31] In our case, the matching between the r_X/r_{Ln} ratio is considerably modified driving the symmetry loss. It involved in $Nd_4O_4(GeO_4)$ two Nd atoms (i.e. Nd1 and Nd2 figure 2b)) located on crystallographic sites with local symmetry *m* out of the mirror plane perpendicular to *c*-axis compared to a single La1 located on a *mm* site, and to the tilting of the GeO_4 tetrahedra. The higher symmetry of the title compound comes together with the location of V^{5+} on a *mm* site, compared to *m* for the twisted Ge^{4+} ions. This difference of symmetry is responsible for different structural complexity as expressed by the Shannon information's content per atom and per unit cell. [32] These values, calculated using the ToposPro software [33], showed a larger structural complexity for the low-symmetric Nd-based structure (I_G = 4.24 bits/atom, $I_{G,total}$ = 220.42 bits/cell) than La-based structure ((I_G = 2.93 bits/atom, $I_{G,total}$ = 76.21 bits/cell) putting both compounds in a very common area in terms of complexity taking into account the complexity distribution reported for inorganic structure database. [34]

To probe potential symmetry loss at low temperature, XRD data of the same La-based single crystal were collected at 100K. Results of the refinement are presented in Table S1. Apart from the thermal contraction no sign of phase transition was evidenced.

Powder synthesis

A powder of $PbLa_3O_4(VO_4)$ was then synthesized from a mixture of PbO, $La(OH)_3$ and V_2O_5, finely grinded in an agate mortar. The sample was then successively heated at 600° and 900° in an alumina crucible. Several intermediate grindings were necessary until achievement of a phase almost pure (additional small peak at 26° figure S1) assigned to $LaVO_4$). The lattice parameters refined from the powder diffraction pattern (using JANA 2006 software [35]) led to a= 5.8812(3)Å, b= 17.9429(9)Å and c= 7.9014(4)Å which is in good agreement with those refined from the single crystal data.

Temperature dependent XRDP study.

The stability in temperature was studied at high temperature by Differential Thermal Analyses (DTA) and *in situ* High Temperature X-Ray Diffraction. Figure S2a) shows the typical DTA plot obtained for $PbLa_3O_4(VO_4)$ under air from RT to 800°C at a heating rate of 10°C.min^{-1}. A small, endothermic peak is observed on heating at 310°C. In agreement with results of ref [36], it was assigned to the $LaVO_4$ minor impurity. We also checked the sample by *in situ* HTXRD under air in similar conditions. The refinement of both unit cell parameters and volume allowed the determination of the linear thermal expansion coefficients: α_V= 35.3, α_a= 9.8, α_b= 16.9 and α_c= 8.3 (10^6. K^{-1}). The thermal expansion of this material is twice higher along *b*-axis (so anisotropic), matching well with the rigid oxo-centered units and 2D-lattice growing in the (a,b) plane. In contrast we expect the more ionic external Ln/Pb---O-V to vary more strongly upon heating.

Infrared spectroscopy

The infrared spectrum of $PbLa_3O_4(VO_4)$ is displayed figure S3, where bands between 700 and 800cm^{-1} are assigned to $[VO_4]^{3-}$ vibrations mode, the one around 440cm^{-1} to La-O and at 490 cm^{-1} and 840cm^{-1} to Pb-O vibrations. [37] [38] The main information arise from absence of peaks around 3600cm^{-1}, usually attributed to O-H vibrations, excluding the presence of hydroxyl groups or water molecules, although lanthanum oxides are known to be easily decomposable by hydroxylation or incorporation of water molecules at the surface.

Ln substitution

The possibility to substitute La^{3+} by Nd^{3+} was checked using the same experimental route than the one described above starting from Nd_2O_3 oxide precursors. Despite several attempts changing parameters during the solid-state synthesis (temperature, precursors, time…), $PbNd_3O_4(VO_4)$ was systematically accompanied with a small amount of $NdVO_4$ (estimated to 8% in weight) (figure S4) The refined lattice parameters are a= 5.7760(1)Å, b= 17.7534(3)Å and c= 7.7330(2)Å.

Optical properties: UV-vis spectroscopy

Figure 3a) shows the UV-vis diffuse reflectance spectrum (DRS) of the La-compound between 300 and 800nm (or 4.13 and 1.55eV). One can note a broad absorption edge below 3.3eV with a bump at lower energy (around 2.6eV). This corresponds to an absorption in blue-green responsible for the orange colour of the compound (V3d transitions). Then, this broad absorption edge includes Pb^{2+}, La^{3+} and VO_4 interactions. However its continuous decay above the fermi level shows the important contribution of defect levels.

Concerning the Nd-compound, the global behaviour of the UV visible absorbance is almost similar to La-compound. In that case, the breaking occurs around 3.05V and the bandgap is estimated to be around 2,85eV, which also justifies the pale green colour of the powder. In addition, the peaks observed at low energy are assigned to the main f-f transitions of Nd as detailed on figure 3.a).

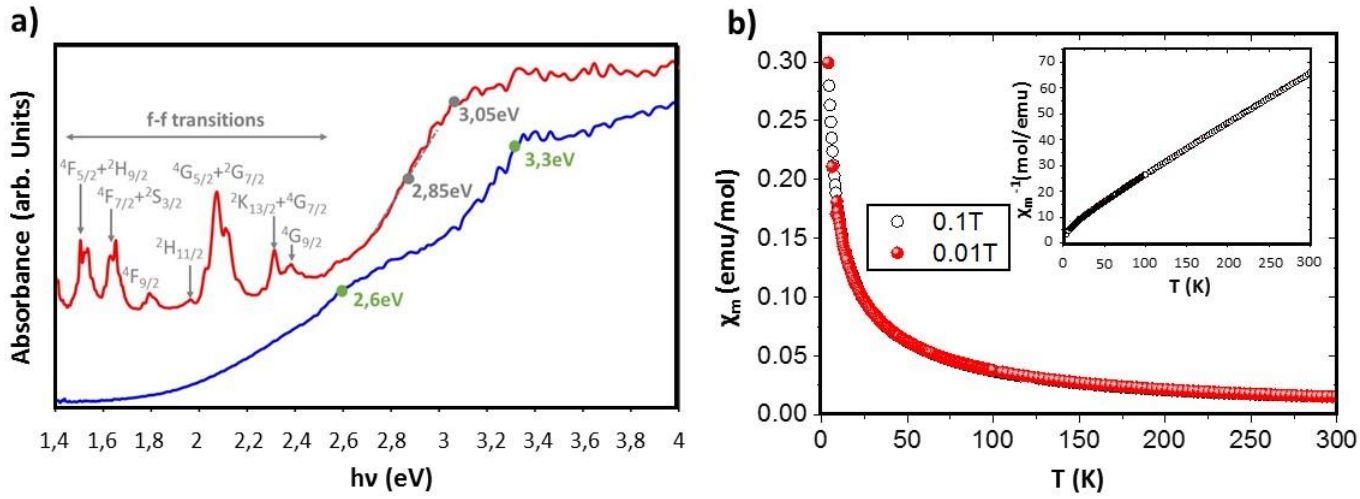

Figure 3. a) Optical absorption spectra for $PbLa_3O_4(VO_4)$ (blue) and $PbNd_3O_4(VO_4)$ (red). The f-f transitions of Nd^{3+} cations are detailed, b) Molar magnetic susceptibility of $PbNd_3VO_8$ as function of the temperature for 2 applied magnetic field (0.1 and 0.01T). In the inset is shown the inverse of susceptibility as function of the temperature, the linear part corresponds to the Curie Weiss domain.

Magnetic properties

The magnetic susceptibility of polycrystalline $PbNd_3O_4(VO_4)$ was measured under magnetic fields of 0.01T and 0.1T using field cooling and zero field cooling procedures, from room temperature down to 4K (figure 3.b)). In this compound the magnetic moments are given by the three Nd^{3+} per FU.

Within experimental resolution, all curves are observed to be superimposed, in agreement with a pure paramagnetic regime and in absence of magnetic ordering. As shown in the inset of figure 3.b), a Curie-Weiss behaviour is observed for $T \gtrsim 50K$, and fitting the linear part of $\chi^{-1}(T)$ gives a molar Curie constant C_{mol}= 5.02emu.mol^{-1}.K, giving an effective moment $\mu_{eff} \approx (8.C_{mol})^{1/2} \approx 6.3\ \mu_B$/f.u. (i.e. gives 3.64 μ_B/Nd) and a Weiss temperature $\theta_W \approx -38K$, *a priori* indicating moderate antiferromagnetic interactions. It is in very good agreement with the free ion value of Nd^{3+} which is $4f^3$ (S=3/2, L=6, J=8/2, $\mu_{eff}=(2g_J^2 J(J+1))^{1/2}\mu_B \approx 3.62\mu_B$). The consideration of a small amount of $NdVO_4$ impurity ($NdVO_4$ is also a paramagnet with Nd^{3+} ion) should not change significantly the experimental value.
Note that the deviation from a simple Curie Weiss law observed at low temperature $T \lesssim 50K$ is very similar to what was previously reported in other paramagnetic oxides containing Nd^{3+}. This deviation was shown to be due to splitting of the ion ground state by the crystal field. [39] It follows that the negative Weiss constant that we inferred from the Curie-Weiss fitting of the experimental data reflects likely such crystal field effects of the Nd^{3+} ground state and not antiferromagnetic interactions.

Conclusions

In an attempt to find new inorganic phosphors able to host emitters for white LEDs applications a new lanthanum lead vanadate was isolated and fully characterised from a structural point of view. Its structure is similar to $Nd_4O_4(GeO_4)$, already reported in the literature. This crystal structure is flexible as it may host different kind of atoms in its cationic backbone and around with different nature of XO_4 tetrahedra. It opens the door to further design of structures, playing both on the nature of atoms and on the size and shape of the layers. Indeed, in the present case, the height of steps is 2x2 but it has been shown in other systems that it can 3x4. [7], [40] This series of materials can thus be tuned in order to build 2D materials from sizable 2D building units. This approach was already successfully applied in the case of Bi-based materials [17], [41] and we believe that it may be extended to La-based materials, after optimization of synthesis routes. Concerning the possibility of introducing emitters, the insertion of neodymium is very promising and opens the door to introduction of other lanthanides and especially Sm^{3+}, Eu^{3+}, Tb^{3+} or mixtures of them.

Experimental Section

Synthesis of I: Single crystals of $PbLa_3O_4(VO_4)$ have been prepared by the flux growth method. A mixture of V_2O_5 (2mmol, Alfa Aesar, 99%), $La(OH)_3$ (1mmol, Alfa Aesar, 99,5%) and PbO (5mmol, Aldrich, 99,9%) was solely ground and loaded into a platinum crucible. The crucible was loaded into a tubular furnace heated to 1000°C for 10 hours. Then the temperature was lowered to 800 °C during 48 hours. Afterwards, the furnace was switched off. Block-shaped orange single crystals of the titled compound were found in large amount.

X-Ray crystallography. A suitable orange crystal of $PbLa_3O_4(VO_4)$ with approximate dimensions 0.023 × 0.047 × 0.072mm3 was selected under polarizing optical microscope and glued on a glass fibre for a single-crystal X-ray diffraction experiment. X-ray intensity data were collected on a Bruker APEX2 CCD 4K area-detector diffractometer using an Incoatec Mo-Kα Microfocus source (λ=0.71073 Å) at room temperature and at 100K. Any important difference is observed between both temperatures and so only the room temperature refinement is presented in this paper. An orthorhombic unit cell with a=5.8858(4)Å, b=17.9380(12)Å, c=7.99079(5)Å and V= 834(10)$Å^3$ was revealed. Several sets of narrow data frames were collected at different values of θ (3.44 to 28.31°), using 0.3° increments of ϕ or ω to obtain a full sphere of three-dimensional data. Data reduction was accomplished using SAINT V7.53a. [42] The substantial redundancy in data allowed the use of a semi-empirical absorption correction (SADABS [43]), on the basis of multiple measurements of equivalent reflections. The systematic absences of reflections are consistent with the space group *Cmcm*. The structures were solved using SUPERFLIP [44] and refined by full-matrix least-squares procedures on F using JANA2006 program. [35] The final R value of 2.37% was obtained for 578 unique reflections with I>3σ(I) with all structure refinement details given Table 1.

Powder X-Ray diffraction was performed at room temperature in the angular range 10–80° with a scan step width of 0.02° using a D8 Advance Bruker AXS diffractometer in Bragg Brentano geometry equipped with a 1D LynxEye detector with a CuKα1,2 radiation (λ = 1.540598 Å and 1.54439Å). Full pattern matching was performed using JANA2006. [35] The X-ray thermodiffraction experiments were also performed with a diffractometer D8 ADVANCE (Bruker-AXS) in Bragg Brentano geometry and equipped with a 1D LynxEye detector. The patterns were measured in air every 100°C from RT to 850°C (heating rate of 10°C.min^{-1}) using an Anton-Paar XRK900 furnace.

Infrared spectra was measured on a Perkin Elmer Spectrum Two spectrometer between 4000 and 400 cm^{-1}, equipped with a diamond attenuated total reflectance (ATR) accessory.

UV/Vis spectra were collected at room temperature using a Perkin Elmer Lambda 650 spectrophotometer in the 300-800nm range. Before the measurement, the blank was measured using $BaSO_4$ (standard for 100% reflectance) in order to calibrate the device.

Magnetic properties were measured using a Squid MPMS (Magnetic properties measurement system, Quantum Design) in dc mode. The temperature range was 4-300K and magnetic field values were 0.1 and 0.01T.

Acknowledgement

This work was carried out under the framework of the Multi-InMaDe project supported by the ANR (Grant ANR 2011-JS-08 00301). The Fonds Européen de Développement Régional (FEDER), CNRS, Région Nord Pas-de-Calais, and Ministère de l'Education Nationale de l'Enseignement Supérieur et de la Recherche are acknowledged for funding the X-ray diffractometers. The author thank J.F. Blach for fruitful discussion and Laurence Burylo for X-ray diffraction.

References

[1] N.C. George, K.A. Denault and R. Seshadri, R, Annu. Rev. Mat. Res., 43(1) (2013) 481-501.
[2] L. Chen, C.-C. Lin, C.-W. Yeh, and R.-S. Liu, Materials, 3(3) (2010) 2172–2195.
[3] S. Pimputkar, J. S. Speck, S. P. DenBaars, and S. Nakamura, Nat. Photonics, 3(4) (2009) 180–182.
[4] M. Derbel, A. Mbarek, G. Chadeyron, M. Fourati, D. Zambon, and R. Mahiou, J. Lumin., 176 (2016) 356–362.
[5] M. Janulevicius, P. Marmokas, M. Misevicius, J. Grigorjevaite, L. Mikoliunaite, S. Sakirzanovas, A. Katelnikovas, Sci. Rep., 6 (2016) 26098.
[6] E. Pavitra, G. S. R. Raju, J. Y. Park, L. Wang, B. K. Moon, and J. S. Yu, Sci. Rep., 5 (2015) 10296.
[7] M. Colmont, L. Palatinus, M. Huvé, H. Kabbour, S. Saitzek, N. Djelal, P. Roussel, Inorg. Chem., 55(5) (2016) 2252–2260.
[8] M. Colmont, S. Saitzek, A. Katelnikovas, H. Kabbour, J. Olchowka, and P. Roussel, J. Mater. Chem. C, 4(30) (2016) 7277-7285.
[9] J. Bashir and M. N. Khan, Mater. Lett., 60(4) (2006) 470–473.
[10] H. Kasatani, T. Umeki, and H. Terauchi, J. Phys. Soc. Jpn., 61(7) (1992) 2309–2316.
[11] R. D. Shannon and C. Calvo, Can. J. Chem., 51(1) (1973) 70–76.
[12] D. E. Bugaris and H.-C. zur Loye, Angew. Chem. Int. Ed., 51(16) (2012) 3780–3811.
[13] S. V. Krivovichev, O. Mentré, O. I. Siidra, M. Colmont, and S. K. Filatov, Chem. Rev., 113(8) (2013) 6459–6535.
[14] M. Colmont, G. Bucataru, A. Borowiec, M. Capron, F. Dumeignil, M. Huvé, F. Capet, F. Damay, O. Mentré, P. Roussel, Dalton Trans, 44(32 (2015) 14444–14452.
[15] O. I. Siidra, S. V. Krivovichev, and S. K. Filatov, Z. Für Krist., 223 (2008) 01–02.
[16] M. Colmont, M. Huvé, E. M. Ketatni, F. Abraham, and O. Mentré, J. Solid State Chem., 176(1) (2003) 221–233.
[17] D. Endara, M. Colmont, M. Huvé, F. Capet, J. Lejay, P. Aschehoug, O. Mentré, Inorg. Chem., 51(17) (2012) 9557–9562.
[18] V. M. Kovrugin, O. I. Siidra, M. Colmont, O. Mentré, and S. V. Krivovichev, Mineral. Petrol., 109(4) (2015) 421–430.
[19] M. Lü, A. Aliev, J. Olchowka, M. Colmont, M. Huvé, C. Wickleder, O. Mentré, Inorg. Chem., 53(1) (2014) 528–536.
[20] A. Aliev, J. Olchowka, M. Colmont, E. Capoen, C. Wickleder, and O. Mentré, Inorg. Chem., 52(15) (2013) 8427–8435.
[21] H. Effenberger, *Monatshefte Für Chem. Chem. Mon.*, 117(10) (1986) 1099–1106.
[22] B. V. Merinov, B. A. Masimov, D. N. Dem'yanets, and N. V. Belov, Dokl. Akad. Nauk, 241 (1978) 353–356.
[23] R. D. Purohit, A. Chesnaud, A. Lachgar, O. Joubert, M. T. Caldes, Y. Piffard, L. Brohan, Chem. Mater., 17(17) (2005) 4479–4485.
[24] O. I Siidra, S.V. Krivovichev, T. Armbruster, W. Depmeier, Inorg. Chem. 46 (2007) 1523–1525
[25] A. Verbaere, R. Marchand, and M. Tournoux, J. Solid State Chem., 23(3–4) (1978) 383–390.
[26] P. P. Ewald, Ann. Phys., (1924) 253–287.
[27] O. I. Siidra, M. Gogolin, E. A. Lukina, H. Kabbour, R. S. Bubnova, O. Mentré, A. A. Agakhanov, S. V. Krivovichev, M. Colmont, T. Gesing, Inorg. Chem., 54(23) (2015) 11550–11556.
[28] E. Morin, G. Wallez, S. Jaulmes, J. C. Couturier, M. Quarton, J. Solid State Chem., 137(2) (1998) 283–288.
[29] E. M. Ketatni, B. Mernari, F. Abraham, and O. Mentre, J. Solid State Chem., 153(1) (2000) 48–54.
[30] F. Abraham, E. M. Ketatni, G. Mairesse, and B. Mernari, Eur. J. Solid State Inorg. Chem., 31(4) (1994) 313–323.

[31] O. Mentré, E. M. Ketatni, M. Colmont, M. Huvé, F. Abraham, and V. Petricek, J. Am. Chem. Soc., 128(33) (2006) 10857–10867.
[32] R. D. Shannon, Acta Crystallogr. Sect. A, 32(5) (1976) 751–767.
[33] V. A. Blatov, A. P. Shevchenko, and D. M. Proserpio, Cryst. Growth Des., 14(7) (2014) 3576–3586.
[34] S. V. Krivovichev, Angew. Chem. Int. Ed., 53(3) (2014) 654–661.
[35] V. Petříček, M. Dušek, and L. Palatinus, Z. Für Krist. - Cryst. Mater., 229(5) (2014) 345-352.
[36] K. Gaur, H.B. Lal, J. Mater. Sci., 19 (1984) 3325-3329.
[37] R. Newman, J. Am. Inst. Conserv., 19(1) (1979) 42–62.
[38] A. He, F. Zhou, F. Ye, Y. Zhang, X. He, X. Zhang, R. Guo, X. Zhao, Y. Sun, M. Huang, Q. Li, Z. Yang, Y. Xu, J. Wu, *J. Spectrosc.*, 2013 (2013) 1–6.
[39] C. Cascales, R. Sáez-Puche, P. Porcher, J. Solid State Chem., 114(1) (1995) 52–56.
[40] J. Zhu, W. D. Cheng, D. S. Wu, H. Zhang, Y. J. Gong, H. N. Tong, D. Zhao, Inorg. Chem., 46(1) (2007) 208–212.
[41] M. Huvé, M. Colmont, J. Lejay, P. Aschehoug, and O. Mentré, Chem. Mater., 21(17) (2009) 4019–4029.
[42] *SAINT: Area-Detector Integration Software*. Madison: Siemens Industrial Automation, Inc., (1996).
[43] *SADABS: Area-Detector Absorption Correction*. Madison: Siemens Industrial Automation, Inc., (1995).
[44] L. Palatinus and G. Chapuis, J. Appl. Crystallogr., 40(4), (2007) 786–790.

Entry for the Table of Contents

Undulated oxocentered layes in $PbLn_3O_4(VO_4)$ (Ln= La and Nd) and relationship with $Nd_4O_4(GeO_4)$.

Marie Colmont*[1], Olivier Mentré[1], Natacha Henry[1], Alain Pautrat[2], Bastien Leclercq[1], Frédéric Capet[1], Nora Djelal[1] and Pascal Roussel[1]

This paper reports the crystal structure of $PbLn_3O_4(VO_4)$, (Ln= La and Nd) and its structural relationship with $Nd_4O_4(GeO_4)$. Optical and magnetic properties were also studied when appropriated.